Defense Threat Reduction Agency
8725 John J. Kingman Road, MS-6201
Fort Belvoir, VA 22060-6201

DTRA-TR-14-73

TECHNICAL REPORT

Powder Processing of Amorphous Tungsten-bearing Alloys and Composites

Approved for public release; distribution is unlimited.

March 2015

HDTRA1-11-1-0062

Christopher Schuh et al.

Prepared by:
Massachusetts Institute of Technology
77 Massachusetts Ave
Cambridge, MA 02139

DESTRUCTION NOTICE:

Destroy this report when it is no longer needed.
Do not return to sender.

PLEASE NOTIFY THE DEFENSE THREAT REDUCTION AGENCY, ATTN: DTRIAC/ J9STT, 8725 JOHN J. KINGMAN ROAD, MS-6201, FT BELVOIR, VA 22060-6201, IF YOUR ADDRESS IS INCORRECT, IF YOU WISH THAT IT BE DELETED FROM THE DISTRIBUTION LIST, OR IF THE ADDRESSEE IS NO LONGER EMPLOYED BY YOUR ORGANIZATION.

REPORT DOCUMENTATION PAGE

Form Approved
OMB No. 0704-0188

1. REPORT DATE *(DD-MM-YYYY)*	**2. REPORT TYPE**	**3. DATES COVERED** *(From - To)*
00-03-2015	Technical	August 22, 2011 - August 21, 2014

4. TITLE AND SUBTITLE

Powder Processing of Amorphous Tungsten-bearing Alloys and Composites

5a. CONTRACT NUMBER
HDTRA1-11-1-0062

5b. GRANT NUMBER

5c. PROGRAM ELEMENT NUMBER

6. AUTHOR(S)

Christopher Schuh
Megan Frary
Brian Schuster

5d. PROJECT NUMBER

5e. TASK NUMBER

5f. WORK UNIT NUMBER

7. PERFORMING ORGANIZATION NAME(S) AND ADDRESS(ES)

Massachusetts Institute of Technology
77 Massachusetts Ave
Cambridge, MA 02139

8. PERFORMING ORGANIZATION REPORT NUMBER

9. SPONSORING / MONITORING AGENCY NAME(S) AND ADDRESS(ES)

Defense Threat Reduction Agency
8725 John J. Kingman Road STOP 6201
Fort Belvoir, VA 22060
PM/Suhithi Peiris

10. SPONSOR/MONITOR'S ACRONYM(S)
DTRA

11. SPONSOR/MONITOR'S REPORT NUMBER(S)
DTRA-TR-14-73

12. DISTRIBUTION / AVAILABILITY STATEMENT

Approved for public release; distribution is unlimited.

13. SUPPLEMENTARY NOTES

14. ABSTRACT

The goal of this project was to develop a W-based amorphous-crystalline composite for penetrator applications. The composite was to have high strength, toughness, abrasion resistance, tailorable density, and a propensity for shear localization. Our year 3 tasks, as laid out in the project proposal, were to:
1) Consolidate amorphous or nanocrystalline powder blends
2) Mechanical testing
3) Ballistic testing

15. SUBJECT TERMS

Tungsten Composites Amorphous Powder

16. SECURITY CLASSIFICATION OF:			**17. LIMITATION OF ABSTRACT**	**18. NUMBER OF PAGES**	**19a. NAME OF RESPONSIBLE PERSON**
a. REPORT	**b. ABSTRACT**	**c. THIS PAGE**	UU	25	Suhithi Peiris
Unclassified	Unclassified	Unclassified			**19b. TELEPHONE NUMBER** *(include area code)* 703-767-4732

Standard Form 298 (Rev. 8-98)
Prescribed by ANSI Std. Z39.18

CONVERSION TABLE

Conversion Factors for U.S. Customary to metric (SI) units of measurement.

MULTIPLY →	BY →	TO GET
TO GET ←	BY ←	DIVIDE
angstrom	1.000 000 x E -10	meters (m)
atmosphere (normal)	1.013 25 x E +2	kilo pascal (kPa)
bar	1.000 000 x E +2	kilo pascal (kPa)
barn	1.000 000 x E -28	meter^2 (m^2)
British thermal unit (thermochemical)	1.054 350 x E +3	joule (J)
calorie (thermochemical)	4.184 000	joule (J)
cal (thermochemical/cm^2)	4.184 000 x E -2	mega joule/m^2 (MJ/m^2)
curie	3.700 000 x E +1	*giga bacquerel (GBq)
degree (angle)	1.745 329 x E -2	radian (rad)
degree Fahrenheit	$t_k = (t^of + 459.67)/1.8$	degree kelvin (K)
electron volt	1.602 19 x E -19	joule (J)
erg	1.000 000 x E -7	joule (J)
erg/second	1.000 000 x E -7	watt (W)
foot	3.048 000 x E -1	meter (m)
foot-pound-force	1.355 818	joule (J)
gallon (U.S. liquid)	3.785 412 x E -3	meter^3 (m^3)
inch	2.540 000 x E -2	meter (m)
jerk	1.000 000 x E +9	joule (J)
joule/kilogram (J/kg) radiation dose absorbed	1.000 000	Gray (Gy)
kilotons	4.183	terajoules
kip (1000 lbf)	4.448 222 x E +3	newton (N)
kip/$inch^2$ (ksi)	6.894 757 x E +3	kilo pascal (kPa)
ktap	1.000 000 x E +2	newton-second/m^2 ($N-s/m^2$)
micron	1.000 000 x E -6	meter (m)
mil	2.540 000 x E -5	meter (m)
mile (international)	1.609 344 x E +3	meter (m)
ounce	2.834 952 x E -2	kilogram (kg)
pound-force (lbs avoirdupois)	4.448 222	newton (N)
pound-force inch	1.129 848 x E -1	newton-meter (N-m)
pound-force/inch	1.751 268 x E +2	newton/meter (N/m)
pound-force/$foot^2$	4.788 026 x E -2	kilo pascal (kPa)
pound-force/$inch^2$ (psi)	6.894 757	kilo pascal (kPa)
pound-mass (lbm avoirdupois)	4.535 924 x E -1	kilogram (kg)
pound-mass-$foot^2$ (moment of inertia)	4.214 011 x E -2	kilogram-meter^2 ($kg-m^2$)
pound-mass/$foot^3$	1.601 846 x E +1	kilogram-meter^3 (kg/m^3)
rad (radiation dose absorbed)	1.000 000 x E -2	**Gray (Gy)
roentgen	2.579 760 x E -4	coulomb/kilogram (C/kg)
shake	1.000 000 x E -8	second (s)
slug	1.459 390 x E +1	kilogram (kg)
torr (mm Hg, 0^0 C)	1.333 22 x E -1	kilo pascal (kPa)

*The bacquerel (Bq) is the SI unit of radioactivity; 1 Bq = 1 event/s.

**The Gray (GY) is the SI unit of absorbed radiation.

Grant/Award #: HDTRA1-11-1-0062
PI Name: Christopher Schuh, Megan Frary, Brian Schuster
Organization/Institution: Massachusetts Institute of Technology, Boise State University, Army Research Laboratory
Project Title: Powder Processing of Amorphous Tungsten-bearing Alloys and Composites

What are the major goals of the project?
List the major goals of the project as stated in the approved application or as approved by the agency. If the application lists milestones/target dates for important activities or phases of the project, identify these dates and show actual completion dates or the percentage of completion. Generally, the goals will not change from one reporting period to the next. However, if the awarding agency approved changes to the goals during the reporting period, list the revised goals and objectives. Also explain any significant changes in approach or methods from the agency approved application or plan.

The goal of this project was to develop a W-based amorphous-crystalline composite for penetrator applications. The composite was to have high strength, toughness, abrasion resistance, tailorable density, and a propensity for shear localization. Our year 3 tasks, as laid out in the project proposal, were to

1) Consolidate amorphous or nanocrystalline powder blends
2) Mechanical testing
3) Ballistic testing

In addition to the tasks listed above, a significant effort was dedicated to a more in-depth investigation of the ultrafine grain crystalline materials developed in year 2. These materials were studied because their strength, density, and propensity for shear localization fulfilled the target material requirements of described in our proposal.

What was accomplished under these goals?
For this reporting period describe: 1) major activities; 2) specific objectives; 3) significant results, including major findings, developments, or conclusions (both positive and negative); and 4) key outcomes or other achievements. Include a discussion of stated goals not met. As the project progresses, the emphasis in reporting in this section should shift from reporting activities to reporting accomplishments.

1) Major Activities

Over the past three years, our efforts to develop W-based amorphous-crystalline composites (ACCs) using powder processing followed the outline described in our project proposal. To begin, two sets of W-based alloys were identified using kinetic Monte Carlo and atomistic simulations of mechanical alloying. One set of W-Co-based alloys was expected to amorphize during mechanical alloying; the other set of W-Cr-based alloys was expected to remain crystalline but possess properties enabling its consolidation into fully-dense compacts with tunable grain sizes. Next, powders of each alloy were synthesized using mechanical alloying in a high-energy ball mill. During these milling experiments, we tracked the microstructural evolution of the powder with milling time and adjusted the processing parameters and feedstock powder chemistry to yield powders with the desired properties and microstructures. After fine-tuning the milling schedule and alloy chemistries, a consolidation schedule was developed that enabled the nanocrystalline powder to be consolidated into fully dense compacts with controllable grain sizes. Similar consolidation efforts for the amorphous powder are currently underway. Finally, we investigated the quasi-static and dynamic mechanical properties of compacts made from the nanocrystalline alloy powders. Through all of these characterizations, we found that these compacts' densities and mechanical properties met the main goals of this project. Ballistic testing of these materials has been completed and the data are presently being analyzed.

2/3) Specific Objectives and Significant Results

Simulation-Guided Alloy Design

Our first objective in this project was to develop a set of computational tools that can predict the steady state microstructure of mechanically alloyed powders and can therefore help guide the alloy design process. The two methods that we developed use information regarding a couple's thermodynamics and its constituent elements' mechanical properties to predict whether that couple will remain dual-phase and crystalline, form a crystalline solid solution, or amorphize after long milling times.

One of the tools that we developed is a kinetic Monte Carlo (kMC) simulation of mechanical alloying, which we adapted to account for phase-strength effects on forced chemical mixing. Such simulations capture the competition between deformation-induced mixing and thermally activated diffusion during mechanical alloying, and they can be used to test whether a given couple will chemically homogenize or remain dual-phase during processing. By modifying these simulations to exhibit strain partitioning due to differences in phase strength, we made them better suited to study the mechanical alloying of tungsten-transition metal couples in which interdiffusion during mechanical alloying is, to a good approximation, kinetically suppressed, and structural evolution only proceeds through plastic deformation. Using these simulations, we performed a general, parametric study of the effects of composition, material properties, and processing parameters on the development of a chemically homogeneous alloy. The simulation results can be summarized by dynamical phase diagrams like those shown in Figure 1, which serve to illustrate the ambient milling temperatures and compositions at which a couple with a fractional difference in phase strength, Δ, will homogenize.

From the subset of couples that the kMC simuations indicated would homogenize, we next identified ones that would likely amorphize using a molecular dynamics technique in which the simulation cell is

subjected to a series of deformation operations analogous to the repeated fracturing, plastic straining, and cold-welding experienced by the powders in a high-energy ball mill. In this technique, we first initialize a simulation cell consisting of a bilayer of two pure metals that is similar to the lamellar microstructure of mechanically alloyed powders after short milling times. Next, this starting microstructure is iteratively compressed along one direction while being allowed to expand in the other two and then folded so that its dimensions remains roughly constant. During each of these "strain-and-stack" cycles, we track the simulation cell's microstructure, chemical mixity, and amorphous phase fraction. Figure 2, for example, shows the steady-state atomic structures and corresponding partial radial distribution functions (PRDFs) from a series of $W_{1-x}Fe_x$ simulations. We can gauge if a system amorphizes from its PRDF. For example, between x = 0.25 and 0.86, the steady state structure's PRDF has no crystalline peaks and a split in its second peak with both of these features indicating that these compositions amorphized. By performing these simulations with the tungsten-transition metal couples identified from the kMC simulations, we were able to further down-select couples expected to amorphize and one such couple, W-50Co, was the basis for the amorphous powder described later. Another couple studied using this method, W-10Cr, was expected to remain crystalline but form a homogeneous, BCC solid solution. This material was of interest for use as the toughening, crystalline phase in a W-based ACCs.

Alloy Powder Synthesis and Micromechanical Testing

Guided by the simulations just described, we developed amorphous and nanocrystalline W alloy powders with the respective compositions W-38Co-9Fe-20C and W-7Cr-9Fe, at pct. By developing both alloys simultaneously, we were preparing ourselves to combine them into an ACC. Both powders were made by mechanically alloying elemental feedstock powders in a high-energy ball mill under an ultra-high purity Argon atmosphere, and we monitored both of their structural evolutions with milling time using XRD and TEM. The time series XRD shown in Figure 3, for example, illustrates the gradual homogenization of the W and Cr phases in the W-7Cr-9Fe powder: with increasing milling time, the W and Cr phases' Bragg peaks merged, reflecting a homogenization of the two BCC phases' lattice parameters as the W and Cr dissolved in each other to form a single BCC solid solution.

Similarly, the time series XRD shown in Figure 4 illustrates the gradual amorphization of the W-38Co-9Fe-20C alloy. In this figure, the W Bragg peaks' integrated intensity decreases with milling time while there is a commensurate increase in the amorphous ring's intensity, indicating an increasing volume fraction of amorphous material. The TEM micrographs of the as-milled powder shown in Figure 5 support the XRD results. The black dots in these micrographs are residual, crystalline W nanograins; their decreasing number density with milling time shows that the volume fraction of the amorphous material is increasing. Figures 4 and 5, taken together, demonstrate that the crystalline feedstock powders amorphize during mechanical alloying.

To better assess likely consolidation parameters for the amorphous powder, we studied the alloy's structural evolution and crystallization kinetics as a function of temperature using DSC experiments. In particular, the solid state transformations associated with the exotherms shown in Figure 6a were identified by heating the powder to incrementally higher temperatures, quenching, and then studying the microstructure of the annealed powder using TEM and XRD. These results are summarized by the micrographs in Figures 6b and c. Most important from a materials processing perspective, we found that the crystallization start temperature is 700 °C, placing an upper limit on the allowable sintering temperatures.

Prior to consolidating the powders, we also performed small-scale compression tests on micropillars machined out of individual powder particles. These tests confirmed that the powders possessed our target mechanical properties (e.g., high strength and shear localization). We prepared the pillars by mounting the powder particles in epoxy, cross-sectioning them, and then machining out pillars using a focused ion beam (FIB). The pillars were then loaded in compression in a nanoindenter using a 20 x 20 μm diamond flat punch at an initial strain rate of 10^{-4} s^{-1}. Results from these tests are summarized by the stress-strain curves and post-mortem micrographs of pillars shown in Figures 7a and b. As is evidenced by the engineering stress-strain curves in these Figures, both powders possessed yield strengths in excess of the baseline strength of 2 GPa suggested in our proposal, with the nanocrystalline and amorphous powders failing at stresses ~6.5 and ~5.5 GPa, respectively. What is more, the post-mortem SEM micrographs of the pillars provide unequivocal evidence that both alloys deform by shear localization. For example, there are two shear offsets visible in the micrograph of the amorphous pillar that was loaded to ~5.5 GPa in Figure 7a and each of these shear offsets corresponds to a "pop-in" in that pillar's stress-strain curve.

Consolidation Behavior

Having developed two alloy powders possessing strengths and deformation behaviors that are attractive for penetrator applications, we next consolidated the nanocrystalline and amorphous powders separately using the field-assisted sintering (FAS) equipment at Boise State University. In these FAS studies, we used an 8 mm graphite die and a 100 MPa compaction pressure while systematically varying the soak temperature during consolidation. For the nanocrystalline, W-7Cr-9Fe powder, we varied the soak temperature from 1100 to 1400 °C in increments of 100 °C, and used soak times of 1 and 20 minutes at each temperature. We then measured the porosity, grain size, and microhardness of the compacts consolidated using each set of processing parameters. Figure 8 shows these compacts' stereological porosities as a function consolidation temperature and time to illustrate that holding for just 1 minute at 1200 °C resulted in fully dense compacts. Such low temperature densification is impressive in light of the fact that soak temperatures in excess of 1500 °C are necessary to achieve similar relative densities when consolidating pure W. The compacts' grain size measurements shown in Figure 9 illustrate that this rapid low temperature densification enabled the fully-dense compact to retain an ultrafine grain structure (D ~130 nm). A Hall-Petch plot of the fully dense compacts' microhardnesses shown in Figure 10 illustrates how their microhardnesses conformed to a Hall-Petch scaling with the ultrafine grain compact exhibiting an impressive 13.5 GPa microhardness. We anticipate that the data in Figures 8 to 10 will be of use if we incorporate this crystalline powder into future ACC's because they enable us to predict the grain size and resultant hardness of the crystalline phase for a given consolidation schedule.

A similar set of FAS consolidation experiments using the amorphous powder revealed that soak temperatures several hundred degrees above T_x were necessary to achieve full densification when applying a compaction pressure of 100 MPa. Because increasing the compaction pressure tends to lower the densification onset temperature, we are now in the process of consolidating the amorphous powder using compaction techniques that are capable of much higher stresses and that subject the compact to more shear deformation, which is also expected to promote interparticle bonding.

Quasi-static and Dynamic Mechanical Testing

Since the ultrafine grain W-7Cr-9Fe compact's density of ~17 g/cm^3 and microhardness of 13.5 GPa were on target for the goals of the project, we decided to further investigate this material's quasi-static and dynamic mechanical properties. Micropillar compression tests were used to measure the yield strength and study the deformation behavior of the material. The advantage of micropillar compression tests

over traditional bulk compression tests is that when machining the microcompression pillars, we could avoid pores that can lead to premature failure and so better gauge the material's intrinsic deformation response. Engineering stress–strain curves from several microcompression experiments on this material are shown in Figure 11. The average 0.2 pct offset yield strength measured in these experiments was 5.15 GPa, with apparent hardening to an ultimate engineering stress of about 6 GPa followed by a plateau in the stress–strain response. The plateau was associated with the development of a single shear band within the pillar. An example of a shear offset, captured just before failure at an applied stress level of 6.3 GPa, is shown in the inset of Figure 11.

To better gauge how these materials will perform during penetration, we also performed high strain rate compression experiments using a Kolsky bar setup on bulk cuboidal specimens machined from the compacts. A representative engineering stress versus time curve from a Kolsky bar test conducted at a strain rate of 600 s^{-1} is shown in Figure 12. Note that engineering strain values are not reported because these specimens failed at very low strains, which are difficult to measure accurately with a Kolsky bar system. The specimen was loaded until failure, followed by rapid unloading. Accompanying the stress–time curve are images collected using high-speed videography. The average failure stress was 4.14 GPa, which is in rough agreement with the Tabor estimate based on the measured microhardness value reported earlier (σ_F = H/3 = 13.5/3 GPa = 4.5 GPa).

This material's density, quasi-static and dynamic yield strengths, and propensity for shear localization are all promising for use in kinetic penetrator applications. Therefore, we fabricated quarter-scale rounds from several compacts and are in the process of testing their ballistic performance on concrete targets.

4) Key Outcomes

Over the past three years, we utilized a combination of computational and experimental techniques to develop amorphous and nanocrystalline, W-based alloy powders that can be readily consolidated into fully-dense articles possessing high specific gravities, compressive yield strengths, and propensities for shear localization. Our major accomplishments include:

1. The development of a set of computational tools with which we can predict the steady state microstructure of binary alloys subjected to extensive plastic straining processes such as high-energy ball milling.
2. The synthesis of nanocrystalline and amorphous W alloy powders that possess yield strengths in excess of 4 GPa and exhibit shear localization during micropillar compression testing.
3. The consolidation of the nanocrystalline, W-7Cr-9Fe powder into a 98 pct dense compact with a mean grain size of 130 nm. These compacts exhibited a hardness of 13.5 GPa, a dynamic uniaxial yield strength of 4.14 GPa in Kolsky bar experiments, and signs of structural shear localization during deformation.

If awarded additional option years, our research efforts would be dedicated to optimizing the amorphous powders' consolidation schedule, blending the amorphous and crystalline powders to synthesize ACCS, and investigating more in-depth the ballistic performance of both monolithic amorphous and ACC quarter-scale rounds.

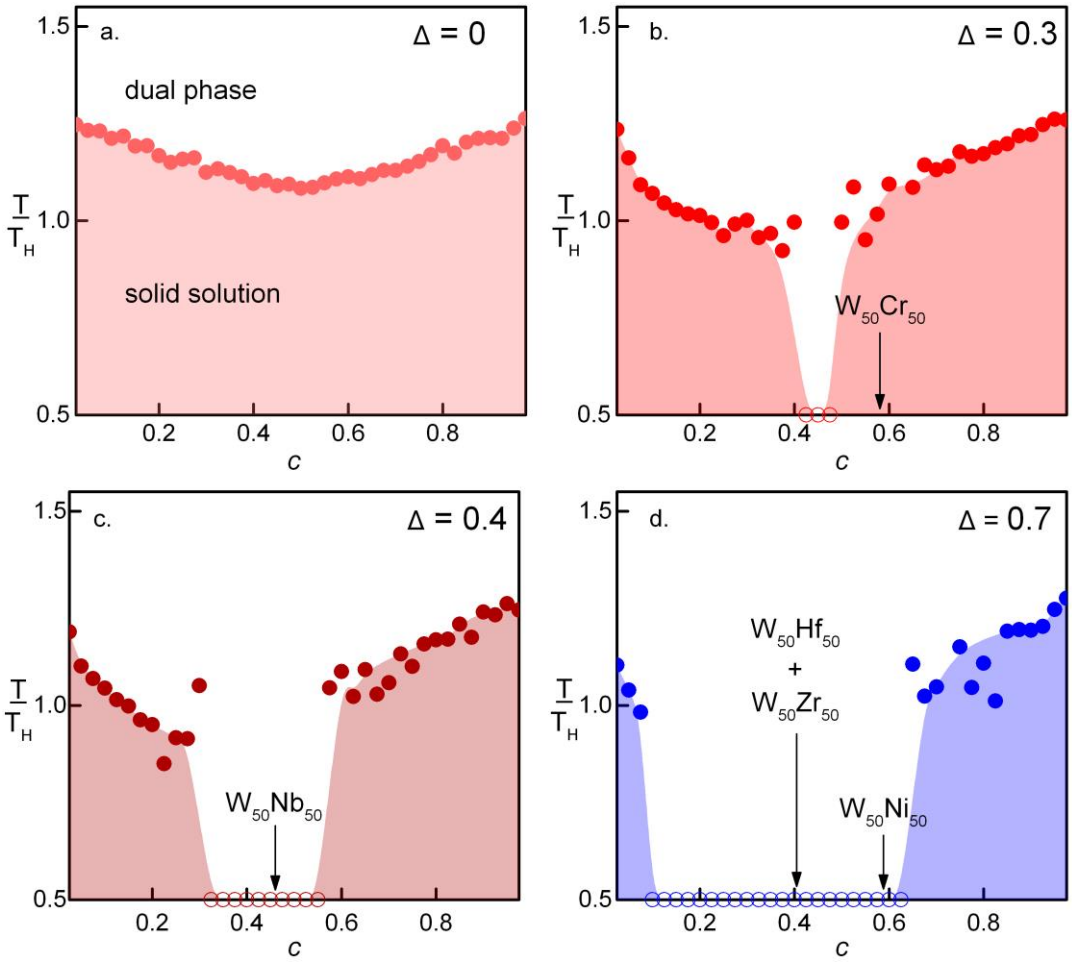

Figure 1 - Dynamical phase diagrams summarizing the kMC simulation results for binary couples with fractional differences in phase strength, Δ, of 0, 0.3, 0.4, and 0.7. The shaded regions below the lines in each panel correspond to the temperatures and compositions at which the various simulations homogenized. With increasing phase strength mismatch, a two-phase region opens up where certain couples remain segregated if they start as such. The open circles on the x-axis indicate compositions that remained dual-phase over the range of temperatures studied. The compositions of several equiatomic W-TM couples that we studied experimentally are placed on these diagrams at their expected locations based on the strength differential in a fine nanocrystalline structure. Agreement between the simulations and experiments was good.

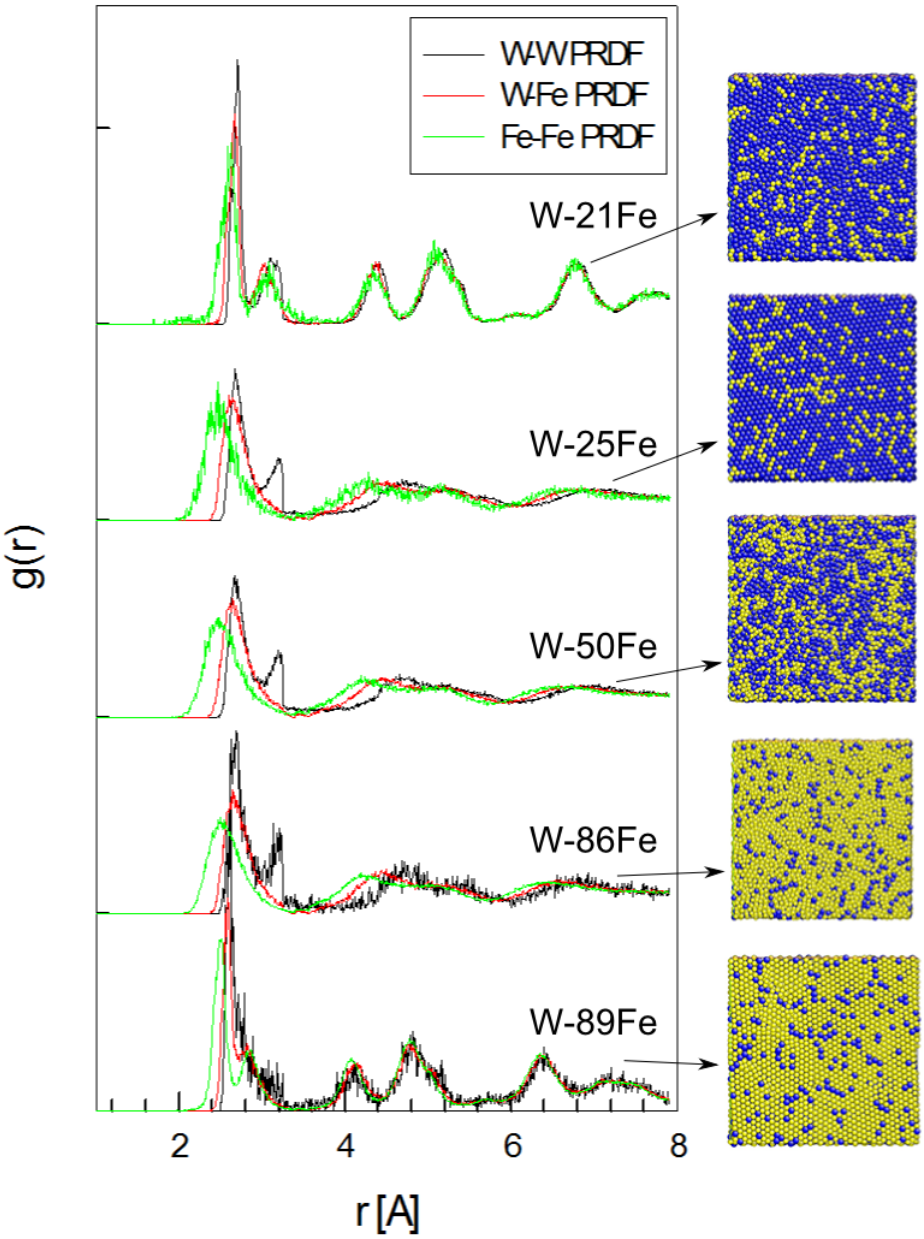

Figure 2 - PRDF and corresponding atomic configurations for several W-Fe couples after four iterations of the "strain-and-stack" technique described in the text. The blue and yellow circles correspond to W and Fe atoms, respectively. The split in the second peak of the PRDF of the $W_{(1-x)}Fe_x$ (x = 25, 50, and 89) couples indicatesthat these compositions have an amorphous structure.

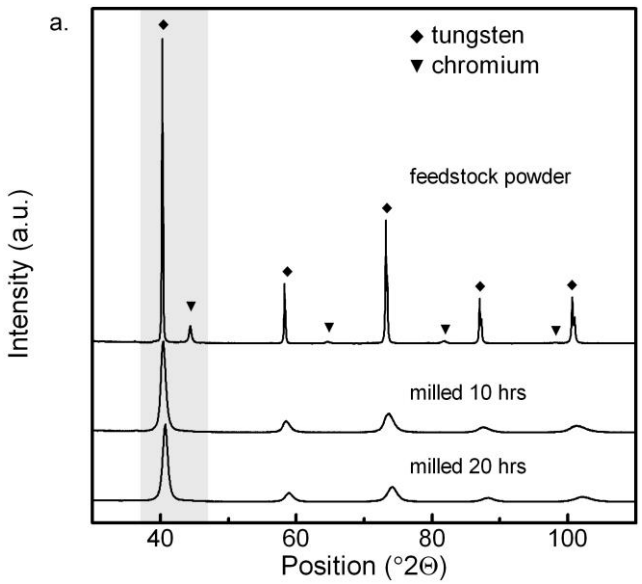

Figure 3 - Set of XRD scans taken from the feedstock and W-7Cr-9Fe powder milled for 10 and 20 hrs. Note the disappearance of the Cr 110 Bragg peak in the highlighted region after 10 hrs of milling. This, along with the change in W lattice parameter, suggests the formation of a solid solution.

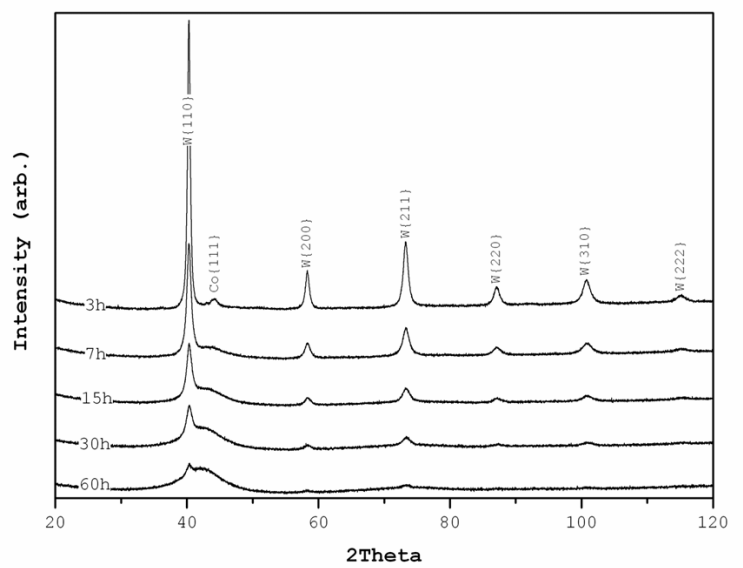

Figure 4 - Time series XRD patterns of the W-Co-C alloy that gradually amorphizes during ball milling. Note the decrease in intensity of the W Bragg peaks is accompanied by an increase in intensity of the amorphous diffraction ring at ~42 °2θ.

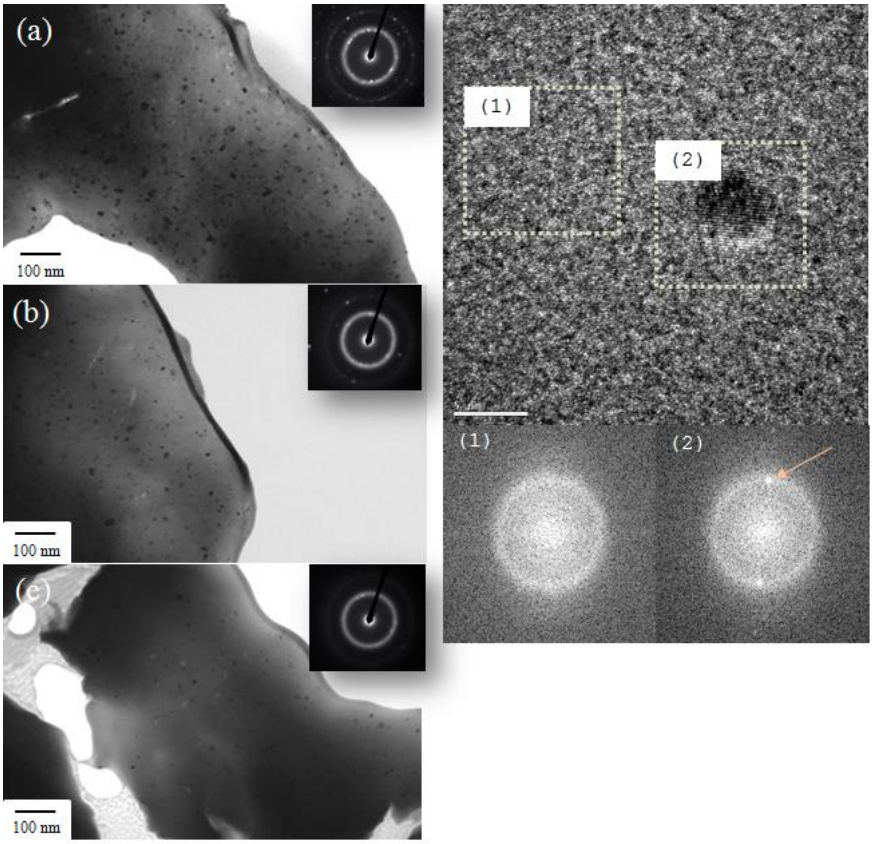

Figure 5 – a-c) Bright Field TEM micrographs with inset diffraction patterns of the W-Co-Fe-C powder milled for 15, 30, and 60 hrs, respectively. The black dots are residual W nanograins, and their decreasing number density with time milled is due to W amorphization. 5d) is a HRTEM image of the 60 hr milled sample. The region labeled (1) is the amorphous matrix and the black region in the box labeled (2) is a W nanograin. FFT of the regions in box (1) and (2) show the diffuse ring and diffraction spots characteristic of amorphous and crystalline materials, respectively.

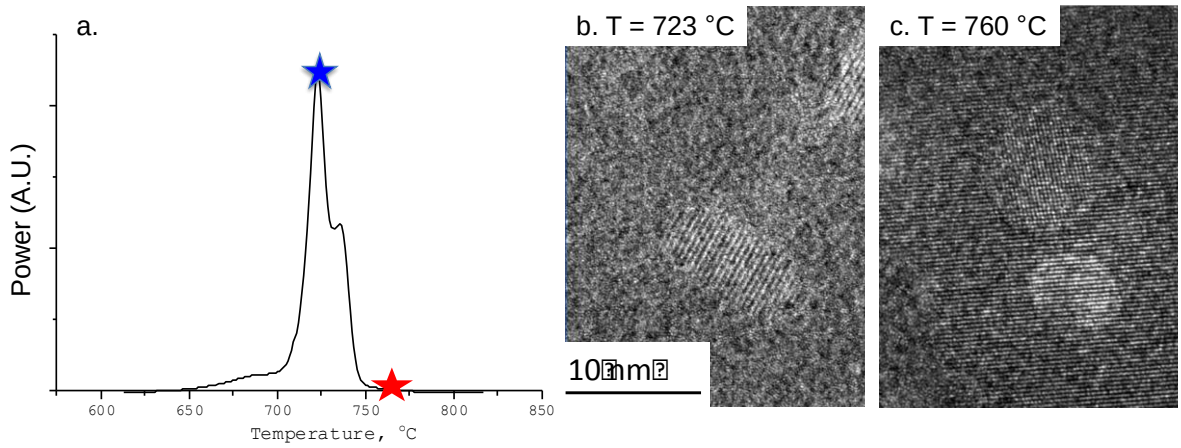

Figure 6 – a) DSC thermogram of the 60 hr milled amorphous alloy. The exothermic reactions at 723 and 734 °C correspond to two separate crystallization reactions. At 723 °C, $W_3[Co,Fe]_3C$ particles precipitate out of the amorphous alloy. These are the regions exhibiting lattice fringes in 6b. At 734 °C, the remaining amorphous material crystallizes into $W_6[Co,Fe]_6C$ as evidenced by the lattice fringes in the matrix shown in 6c.

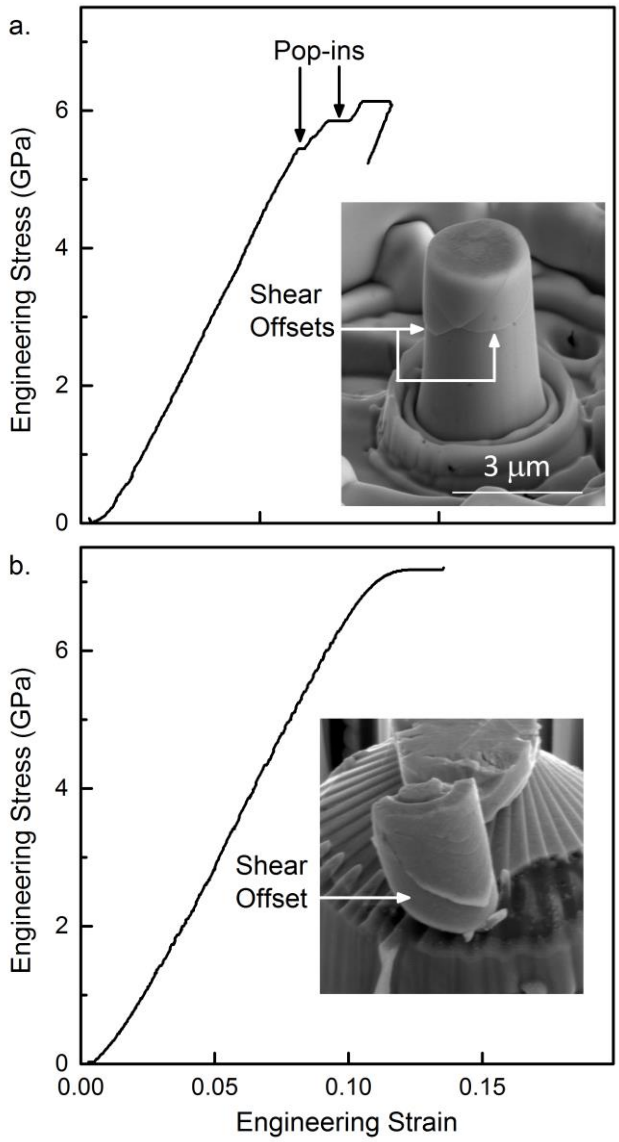

Figure 7 - Engineering stress-strain curves from micropillar compression experiments on the a) amorphous and b) nanocrystalline powders along with inset SEM micrographs of the pillars. The onset of plastic deformation in the amorphous and nanocrystalline powders occurs at stresses of 5.5 and 6.5 GPa, respectively. Note the one-to-one correspondence of shear offsets to pop-ins for the amorphous material in 7a.

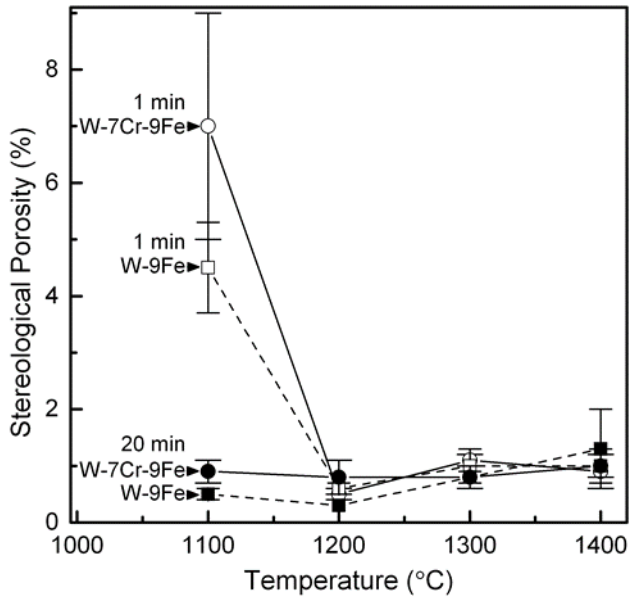

Figure 8 - Stereological porosity of the W-7Cr-9Fe compacts after consolidation experiments at a variety of soak temperatures and two soak times, 1 and 20 minutes.

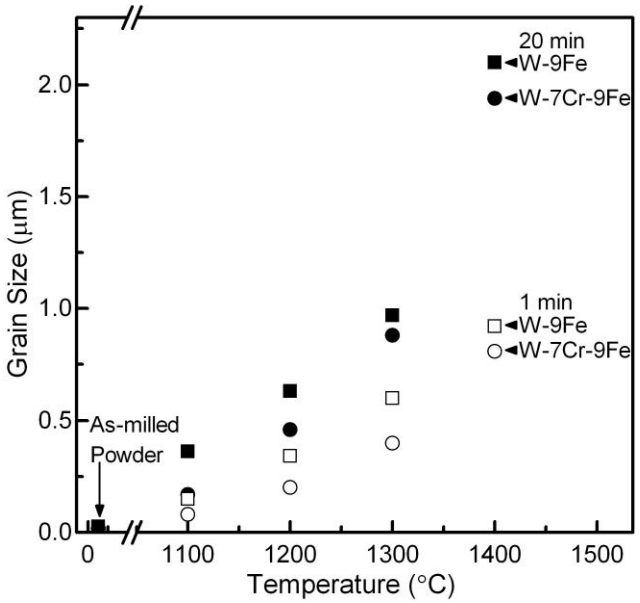

Figure 9 - Grain sizes of compacts made from both alloys and consolidated at various soak temperatures and two soak times, 1 and 20 minutes. Also shown for comparison is the grain size of the as-milled powder.

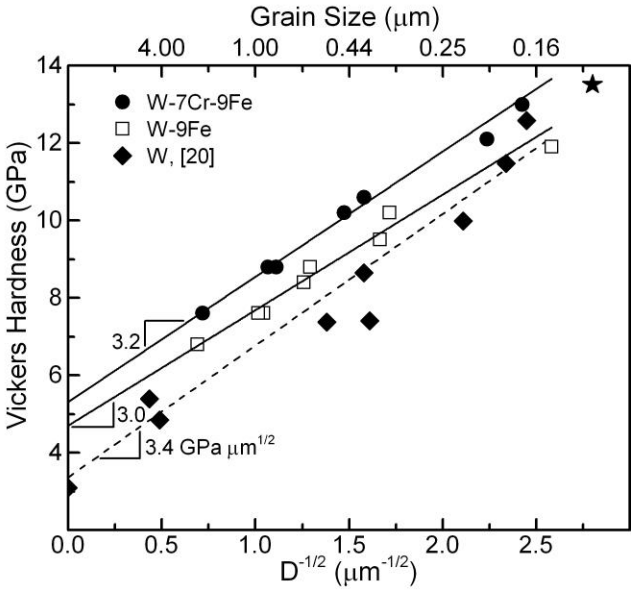

Figure 10 - Hall-Petch plot for compacts made with both alloys, from samples compacted at various times and temperatures to densities in excess of 98%. Data from Vashi *et al*. on nominally pure W compacted to 95% relative density are also presented for comparison. The data point labeled with a star is the hardness of the W-7Cr-9Fe sample consolidated with a grain size of 130 nm.

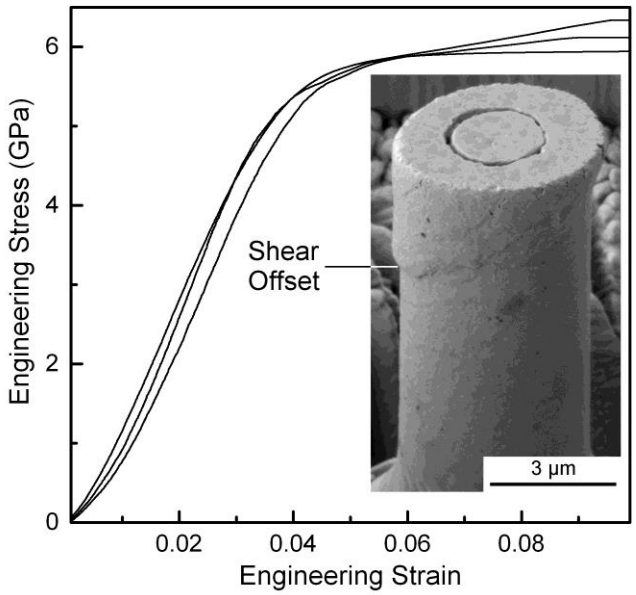

Figure 11 - Engineering stress-strain curves for microcompression experiments on W-7Cr-9Fe compacts consolidated at 1200 °C for 1 minute. The insert shows an SEM micrograph of a micropillar loaded to 6.3 GPa with a shear offset visible on its surface.

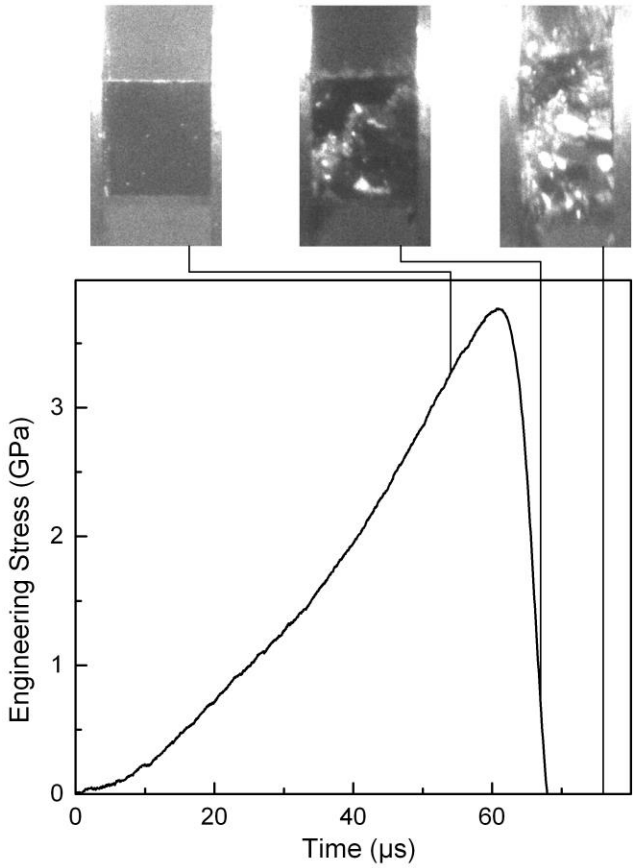

Figure 12 - An engineering stress-time curve from a compressive Kolsky bar test conducted at a strain rate of 600 s^{-1} on W-7Cr-9Fe compacts consolidated at 1200 °C for 1 minute. High speed images correlate to markers on the curve.

What opportunities for training and professional development has the project provided?
If the research is not intended to provide training and professional development opportunities or there is nothing significant to report during this reporting period, state "Nothing to Report." Describe opportunities for training and professional development provided to anyone who worked on the project or anyone who was involved in the activities supported by the project. "Training" activities are those in which individuals with advanced professional skills and experience assist others in attaining greater proficiency. Training activities may include, for example, courses or one-on-one work with a mentor. "Professional development" activities result in increased knowledge or skill in one's area of expertise and may include workshops, conferences, seminars, study groups, and individual study. Include participation in conferences, workshops, and seminars not listed under major activities.

At the Army Research Laboratory, this project provided important professional development opportunities for Dr. Emily Huskins and Ms. Alexandria Will-Cole. Dr. Huskins spent the majority of her two year term at ARL focusing on this DTRA project, and her efforts helped her secure a faculty position at the US Naval Academy in Annapolis, MD starting in the fall of 2014. She will continue to present this work at professional society meetings including TMS and SEM in 2015. Ms. Will-Cole used this project to improve her skills as a young physicist and materials scientist. She learned new characterization techniques including scanning electron microscopy, nanoindentation, energy dispersive spectroscopy and the fundamental links between metal microstructures and mechanical properties. In 2013, Dr. Thomas P. Russell, director of ARL awarded Ms. Will-Cole with top honors for the most outstanding presentation by an undergraduate student for her presentation on "Material Characterization and Mechanical Properties of Ultrafine-Grain Tungsten-Based Alloys."

At Boise State University, two undergraduates and one graduate student were involved with the project. Steven Livers, a graduate student, completed his M.S. in Materials Science and Engineering in December 2013. As a result of his work on this project, Steven developed skills in advanced materials processing, microstructural characterization (including XRD and TEM), and mechanical testing. Steven is now working as an Operations Engineer with the Applied Science Laboratory, a division of Washington State University's Institute for Shock Physics. One of the undergraduates who worked on the project, Megan Beck, is in her third year as part of the Boise State team. Megan also developed strong laboratory skills through her work here. Megan graduated with her B.S. in Materials Science and Engineering in May 2014. She plans to pursue a Ph.D. in Materials Science and Engineering at Northwestern University beginning in September. The second undergraduate who worked on the project, Koyuki Fritchman, had already been working in Dr. Frary's lab for three years. She worked on this project for only a short time, but contributed to the characterization efforts. Koyuki also graduated with a B.S. in Materials Science and Engineering in May 2014.

Zachary Cordero, Braden Knight, and Dr. Kisub Cho were all involved with the research efforts at MIT. Zachary, a third year graduate student, has written two manuscripts on his DTRA-related research and had the opportunity to present the team's work at the 2014 TMS conference. Zachary will also be presenting his work on the application of driven alloy theory to extensively strained materials at the upcoming MS&T conference. Braden Knight is an undergraduate who assisted Zachary in synthesizing and characterizing some of the powders that were subsequently consolidated. This work provided Braden with his first exposure to experimental research and helped him secure an internship at MIT's

Lincoln Laboratories this summer. Dr. Kisub Cho was a postdoctoral associate who contributed to the experimental efforts of the MIT team through March of this past year. The details of Dr. Cho's synthesis of the amorphous W alloy described above are currently being prepared into a manuscript.

How have the results been disseminated to communities of interest?
If there is nothing significant to report during this reporting period, state "Nothing to Report." Describe how the results have been disseminated to communities of interest. Include any outreach activities that have been undertaken to reach members of communities who are not usually aware of these research activities, for the purpose of enhancing public understanding and increasing interest in learning and careers in science, technology, and the humanities.

Most of the experimental results described above have been or are in the process of being disseminated among the metallurgical and materials communities. Details on the synthesis and mechanical properties of the W-7Cr-9Fe alloy were presented at the 2014 TMS conference and were described in a manuscript that was published in Metallurgical and Materials Transactions A. A second manuscript providing guidelines for alloy development using mechanical alloying has been submitted to Acta Materialia and is currently under review.

Results on the development of nanocrystalline and amorphous tungsten alloys have also been disseminated amongst the Army penetrator and warhead material communities. There is considerable interest in these materials as they may offer performance increases over conventional tungsten penetrator materials. Additionally, this research has been used as an outreach mechanism to increase the talent pool of women in science in engineering as it supported the post-doctoral studies by Dr. Emily Huskins and an undergraduate research experience by Ms. Alexandria Will-Cole.

DEPARTMENT OF DEFENSE

DEFENSE THREAT REDUCTION
AGENCY
8725 JOHN J. KINGMAN ROAD
STOP 6201
FORT BELVOIR, VA 22060
ATTN: S. PEIRIS

DEFENSE TECHNICAL
INFORMATION CENTER
8725 JOHN J. KINGMAN ROAD,
SUITE 0944
FT. BELVOIR, VA 22060-6201
ATTN: DTIC/OCA

DEPARTMENT OF DEFENSE CONTRACTORS

QUANTERION SOLUTIONS, INC.
1680 TEXAS STREET, SE
KIRTLAND AFB, NM 87117-5669
ATTN: DTRIAC